

Functional Properties of LSM and LSCF Air Electrodes

Subjects: **Electrochemistry**

Contributor: Elena Filonova , Elena Pikalova

An analysis of the literature data on the electrical, thermal, mechanical, and electrochemical properties of the conventional perovskite-type cathode materials shows that lanthanum strontium manganite ($\text{La},\text{Sr}\text{MnO}_3$) (LSM) fulfills all the requirements for its use in high-temperature SOFCs. However, as the temperature decreases, the use of LSM materials, which are predominantly electronic conductors with a low level of ionic conductivity, becomes unsatisfactory due to their low electrochemical activity for the oxygen reduction reaction (ORR). On the other hand, cobalt-based perovskite materials, including lanthanum strontium cobaltite ferrite ($\text{La},\text{Sr}(\text{Co},\text{Fe})\text{O}_{3-\delta}$) (LSCF), are characterized by superior catalytic activity due to high values of both electronic and ionic conductivity.

SOFC

cathode

air electrode

LSM

LSCF

thermal expansion

conductivity

solid oxide fuel cell

1. Introduction

The development of renewable energy resources, including hybrid power systems [1][2][3][4], is one of the ways for sustainable progress towards decarbonization [5][6][7]. Hybrid energy systems combining solid oxide fuel cells (SOFCs) with heat generators, energy storage devices, internal combustion engines, and solar cells have been intensively designed and manufactured today [4][8][9][10][11]. The progressive trend in the development of SOFCs is to lower the operating temperature, which brings undoubted advantages on the way to the commercialization of these power sources, such as the use of cheaper materials, faster start-up, and increased lifetime due to the reduction of degradation processes. However, challenges arise at low operating temperatures related to the slowing down of electrode reaction kinetics and the increasing ohmic resistance of the electrolyte membrane, resulting in a reduction in the SOFC performance [12][13]. To maintain the electrochemical performance of SOFCs operating at low (LT) and intermediate (IT) temperatures at a satisfactory level, the material optimization has been considered for all construction parts of the SOFC, such as cathodes [14][15][16][17][18][19], anodes [14][19][20][21] and electrolytes [19][22][23][24]. The cathode has been shown to be the major contributor to the electrochemical degradation of the cell [25]. The characterization and performance of the wide range of cathodes can be found in recent reviews [13][26][27][28][29].

An analysis of the literature data on the electrical, thermal, mechanical, and electrochemical properties of the conventional perovskite-type cathode materials shows that lanthanum strontium manganite ($\text{La},\text{Sr}\text{MnO}_3$) (LSM) fulfills all the requirements for its use in high-temperature SOFCs [26][27]. However, as the temperature decreases,

the use of LSM materials, which are predominantly electronic conductors with a low level of ionic conductivity, becomes unsatisfactory due to their low electrochemical activity for the oxygen reduction reaction (ORR) [30][31]. On the other hand, cobalt-based perovskite materials, including lanthanum strontium cobaltite ferrite (La,Sr)(Co,Fe)O_{3- δ} (LSCF), are characterized by superior catalytic activity [32] due to high values of both electronic and ionic conductivity [33]. However, these materials exhibit increased thermal and chemical expansion, which is detrimental to the long-term operation of SOFCs [33][34]. The poor long-term durability of high-temperature electrochemical cells is often caused by the performance degradation phenomenon of the air electrode [35][36][37]. It has been found that the electrochemical performance degradation of the LSM- and LSCF-based air electrodes may include microstructural coarsening [33][38][39], the electrolyte/cathode interface reactions [33][40][41][42], sulfur [43][44][45] and chromium poisoning [44][46][47][48][49], carbon deposition [50][51], and Sr surface segregation [33][35][36][52].

The perceived drawbacks of lanthanum strontium-based cathodes have driven research trends towards alternative solutions to improve their electrochemical performance and durability. A search of the Scopus database using the combination of the keywords "LSM", "SOFC*" and "LSCF", "SOFC*" (with further application of the limits of "cathode*", "cathode materials", "composite cathode*", "cathode polarization", "cathode performance", "electrode*", "oxygen electrode", "electrochemical electrodes") yielded 1141 and 1208 documents respectively for the period of 1996 for LSM and 1998 for LSCF to June of 2023. **Figure 1** and **Figure 2**, generated with the software package VOSviewer version 1.6.19 [53], considering a minimum number of occurrences equal to five author keywords, visualize the maps with topic clusters related to LSM and LSCF as cathode materials for SOFCs, respectively.

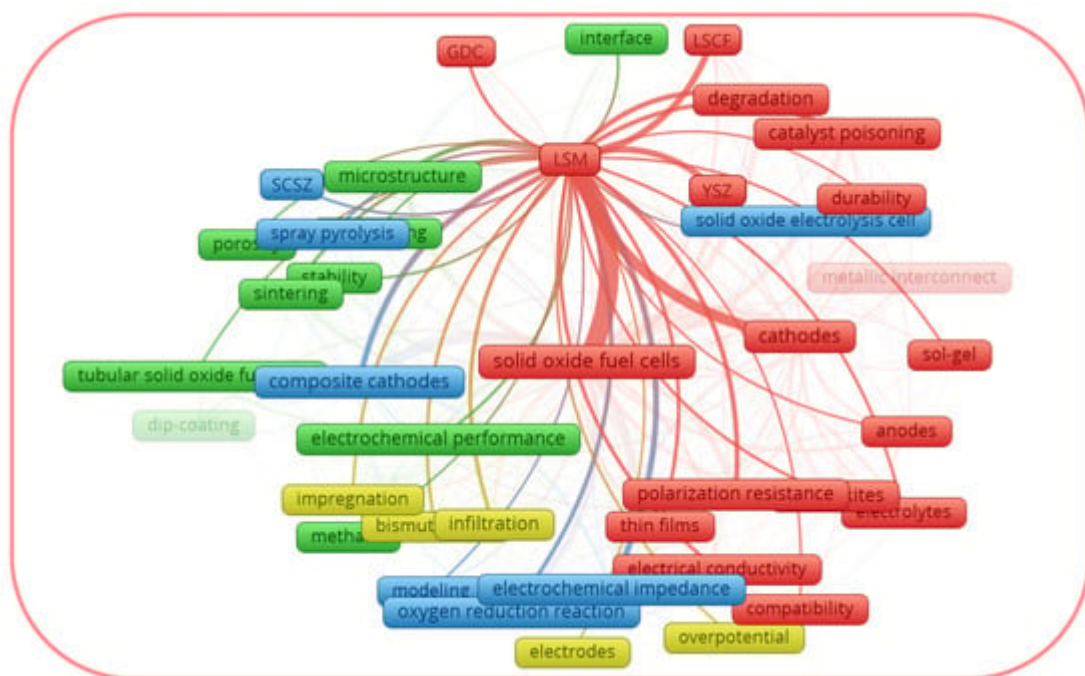


Figure 1. Thematic map of co-occurring author keywords in the Scopus dataset for (La,Sr)MnO₃ (LSM).

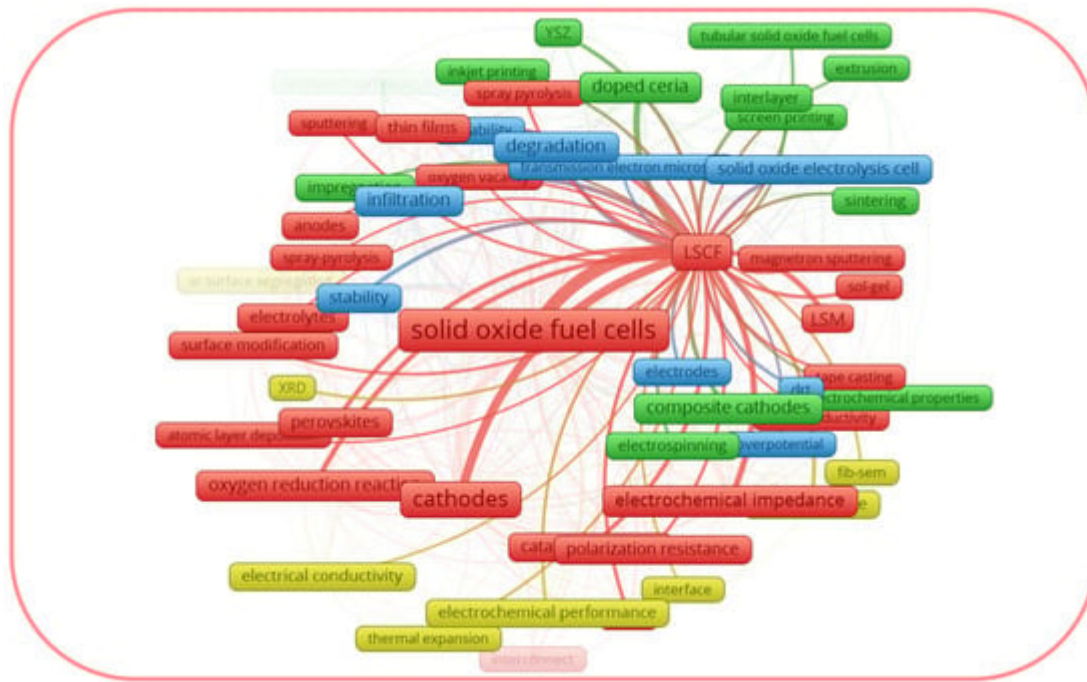


Figure 2. Thematic map of co-occurring author keywords in the Scopus dataset for $(\text{La}, \text{Sr})(\text{Co}, \text{Fe})\text{O}_{3-\delta}$ (LSCF).

From the graphical data shown in **Figure 1**, the author keywords of the documents considered as LSM can be divided into four clusters: the red cluster, focused on the degradation of the cells; the blue cluster, focused on the composite electrodes; the green cluster, focused on the cathode microstructure; and the yellow cluster, focused on the electrode modification using infiltration. Thus, the red cluster generalizes the drawbacks of the LSM cathode, while the other three clusters reflect the strategies to overcome them. From the graphical data shown in **Figure 2**, the author keywords of the documents considered as LSCF can be divided into four clusters, some of which are different from those for LSM. In the case of LSCF, the red, blue, and the green clusters generalize the LSCF performance under the operating conditions of fuel cells, electrolysis cells, and microtubular SOFCs, respectively. The yellow cluster generalizes the interfacial characterization. It is interesting to note that each cluster for LSCF includes the topic of drawbacks and their possible solutions. Thus, the above-mentioned trends justify that the improvement of the activity of LSM and LSCF electrodes remains prominent, and it is important to summarize the thematic studies, provided that the performance of LSM and LSCF has been improved.

2. Key Functional Properties of LSM and LSCF Electrode Materials: Advantages and Drawbacks

The lanthanum strontium manganite $\text{La}_{1-x}\text{Sr}_x\text{MnO}_{3-\delta}$ (LSM), as a representative of complex oxides with a perovskite ABO_3 structure with rhombohedral distortions in the compositional range of $0.2 \leq x < 0.4$ [54][55][56], is known to be used as a material for the fabrication of air electrodes for electrochemical devices operating at low- [57] and intermediate temperatures [30]. On the one hand, this is due to the high level of electronic conductivity σ_e for LSM (corresponding to 200 S cm^{-1} , 250 S cm^{-1} , and 320 S cm^{-1} for $\text{La}_{0.8}\text{Sr}_{0.2}\text{MnO}_{3-\delta}$ (LSM20), $\text{La}_{0.7}\text{Sr}_{0.3}\text{MnO}_{3-\delta}$ (LSM30), and $\text{La}_{0.6}\text{Sr}_{0.4}\text{MnO}_{3-\delta}$ (LSM40), respectively, at 800°C and at $\text{P}_{\text{O}_2} = 1 \text{ bar}$ [58]). Secondly, due to the

closest values of the coefficient of linear thermal expansion (CTE) of the LSM (e.g., for LSM20 — $11.4 \times 10^{-6} \text{ K}^{-1}$ in the range of 50–1000 °C, [59]; for LSM30 — $12.2 \times 10^{-6} \text{ K}^{-1}$ and $13.2 \times 10^{-6} \text{ K}^{-1}$ in the ranges of 200–650 °C and 650–900 °C, respectively, [60]; LSM40 — $12.7 \times 10^{-6} \text{ K}^{-1}$ in the range of 50–1000 °C, [59];) to those for the solid electrolytes perspective for operating in IT-SOFCs and low-temperature SOFCs (LT-SOFCs) [15][22][24][61][62][63]. The CTE values can be mentioned for doped ceria (e.g., for $\text{Ce}_{0.8}\text{Sm}_{0.2}\text{O}_{2-\delta}$ (SDC) — $12.0 \times 10^{-6} \text{ K}^{-1}$ in the range of 25–1000 °C, [64]; for $\text{Ce}_{0.8}\text{Gd}_{0.2}\text{O}_{2-\delta}$ (GDC) — $12.2 \times 10^{-6} \text{ K}^{-1}$ in the range of 50–900 °C, [65]), (Sr,Mg)-doped LaGaO_3 (in general LSGM, e.g., for $\text{La}_{0.8}\text{Sr}_{0.2}\text{Ga}_{0.8}\text{Mg}_{0.2}\text{O}_{3-\delta}$ — $12.1 \times 10^{-6} \text{ K}^{-1}$ in the range of 25–1000 °C, [66]), Sc_2O_3 -stabilized ZrO_2 (ScSZ) (for 8ScSZ — $10.4 \times 10^{-6} \text{ K}^{-1}$ in the range of 30–1000 °C, [67]). In addition, LSM electrodes offer such an important advantage as the improved stability during operation under SOFC and solid oxide electrolysis cell (SOEC) conditions compared to Fe- [48] and Co- [68][69] containing electrodes.

It should be noted that the oxygen diffusion and interfacial heteroexchange parameters for LSM, which is predominantly an electron conductor, are lower than those of materials possessing high mixed oxygen ion and electron conductivity (MIECs), such as cobalt-based perovskites. For example, the oxygen self-diffusion coefficient (D^*) and the oxygen surface exchange coefficient (k) for LSM20 at 800 °C were found to be $4.00 \times 10^{-15} \text{ cm}^2 \text{ s}^{-1}$ and $5.62 \times 10^{-9} \text{ cm s}^{-1}$, respectively, compared to $D^* = 9.87 \times 10^{-10} \text{ cm}^2 \text{ s}^{-1}$ and $k = 6.31 \times 10^{-7} \text{ cm s}^{-1}$ for the $\text{La}_{0.8}\text{Sr}_{0.2}\text{CoO}_{3-\delta}$ MIEC material [70]. The values of the ionic conductivity, σ_i , for LSM are in a range of 10^{-4} – $10^{-7} \text{ S cm}^{-1}$ at 800–1000 °C and decrease significantly in the intermediate temperature range of 600–800 °C [30].

Recently Jiang summarized the literature data regarding the characterization of the oxide materials from the lanthanum strontium cobaltite ferrite $(\text{La},\text{Sr})(\text{Co},\text{Fe})\text{O}_{3-\delta}$ series, and showed that the composition $\text{La}_{0.6}\text{Sr}_{0.4}\text{Co}_{0.2}\text{Fe}_{0.8}\text{O}_{3-\delta}$ (the acronym LSCF will be used from now on), as a representative of MIECs, is the most prominent cathode material used in IT-SOFCs [33]. LSCF, which has a perovskite structure with rhombohedral distortions [71][72], exhibits excellent electrical properties with ionic and electron partial conductivity values reaching approximately $1 \times 10^{-2} \text{ S cm}^{-1}$ and $1 \times 10^2 \text{ S cm}^{-1}$, respectively, at 800 °C [73]. It demonstrates a moderate CTE value equal to $17.5 \times 10^{-6} \text{ K}^{-1}$ in the range of 30–1000 °C [74]. The oxygen self-diffusion and surface exchange coefficients for LSCF amount $5 \times 10^{-7} \text{ cm}^2 \text{ S}^{-1}$ [75] and $6 \times 10^{-6} \text{ cm S}^{-1}$ [76] at 800 °C. It should be noted that due to MIEC conductivity nature and the superior oxygen diffusion properties of LSCF compared to LSM, this material is preferred for use in electrochemical devices operated at lower temperatures, whereas LSM materials are still in high demand for high-temperature applications due to their CTE values being more compatible with electrolyte materials and higher total conductivity values.

The main drawbacks of conventional perovskite electrodes, which lead to the degradation of solid oxide cells during long-term operation, are the segregation of Sr at the electrode surface with the formation of the SrO layer for the LSM- [35][52] and LSCF-based [36][77][78][79][80] cells, and the high interaction of LSM [41][52][81][82][83][84] and LSCF [41][85][86][87][88] with Zr-containing electrolytes to form the SrZrO_3 (SZO) and $\text{La}_2\text{Zr}_2\text{O}_7$ (LZO) phases. In addition, due to the presence of CO_2 in the air, the SrCO_3 carbonate phase was formed on the surfaces of the LSM- [89][90][91] and LSCF- [92][93][94] electrodes. The formation of the same insulating phases limits the oxygen exchange at the electrode–electrolyte interface and reduces the electrocatalytic activity of the LSM [95][96][97][98] and LSCF [77][98][99][100][101][102][103] air electrodes for the ORR, followed by an increase in both the electrode ohmic and polarization

resistances. Similar long-term operation tests have shown that the degradation of cells based on LSM [79] or LSCF [104][105] operating in electrolysis mode was higher than that in fuel cell mode, and when comparing two perovskite electrodes, the long-term durability of LSCF was one step ahead of that of LSM [104][106].

Automated methods developed for the detection of Sr nucleation seeds on the electrode surface [107][108], for the identification of the interlayer width between the perovskite and YSZ layers [109][110], and for the computational design and numerical simulation of the perovskite-based composite electrodes [111][112][113][114] allowed for the suggestion of possible degradation mechanisms and an understanding of the electrode behavior at both the atomic and macroscopic scales. The deposition of protective and non-catalytic layers on the electrode surface has been proposed as a solution to the problems of segregation [115][116][117], contaminant poisoning [118][119][120][121], and sluggish oxygen kinetics [122][123][124][125][126]. The organization of ceria-based buffer layers at the perovskite electrode/YSZ electrolyte interface and the replacement of the zirconium electrolyte in the composite electrode with other ionic conductors, methods widely used for other perovskite electrodes [127][128][129][130][131][132][133], may also help to reduce interactions and increase the activity and long-term stability of LSM [134][135][136] and LSCF [136][137][138][139][140][141][142][143][144][145] electrodes. The high reactivity of the (La, Sr)-containing electrodes with the conventional YSZ electrolyte facilitated extensive investigations of the LSM-based cathodes formed on the SDC [146][147][148][149], GDC [150], SSZ [149][151], LSGM [147], BaZr_{0.8}Y_{0.2}O_{3-δ} (BZY20) [152], La_{9.5}Si₆O_{26.25} [153], and La_{27.44}W_{4.56}O_{55.68} (LWO56) [154] electrolytes as an alternative. The LSCF-based cathodes were formed on the SSZ [155], SDC [156][157], Ce_{0.9}Gd_{0.1}O_{2-δ} (GDC10) [158][159][160], GDC [124][161][162][163][164][165] Y_{0.1}Ce_{0.9}O_{1.95} [166], Nd_{0.2}Ce_{0.8}O_{3-δ} [167], SSZ [168], LSGM [169][170], GDC with LSGM [171], SDC with LSGM [172], BZY20 [173], BaZr_{0.9}Y_{0.1}O_{3-δ} [174], BaZr_{0.8}Yb_{0.2}O_{3-δ} (BZYb) [175], BaCe_{0.7}Zr_{0.1}Y_{0.1}Yb_{0.1}O_{3-δ} (BCZYYb) [176][177][178][179][180], BaCe_{0.7}Zr_{0.1}Y_{0.2}O_{3-δ} (BCZY) [181][182][183], and BaCe_{0.7}Zr_{0.15}Y_{0.15}O_{3-δ} (BCZY15) [184] electrolytes.

The chemical compatibility of the LSM and LSCF electrodes with oxygen-ion and proton-conducting electrolytes and the interdiffusion across the cathode/interlayer/electrolyte interfaces have been extensively observed in the recent reviews of Zhang et al. [41], Khan et al. [42] and Hanif et al. [185]. To briefly summarize the data presented in [41], it could be mentioned that LSM20, in contrast to LSCF, showed good chemical compatibility with La₂₇W₄NbO_{55-δ} up to 1400 °C [186] and with La₁₀Si₅₅Al_{0.5}O_{26.75} at 1300 °C [187], whereas the La-deficient LSM40 did not react with La_{0.9}Sr_{0.1}Ga_{0.8}Mg_{0.2}O_{2.85} (LSGM9182) at 1300 °C [188]. Secondary phases were found to form after sintering of LSM20 with SDC and BaCe_{0.9}Y_{0.1}O_{3-δ} at 1150 °C [189], La-deficient LSM20 with BZY20 and BaCe_{0.8}Y_{0.2}O_{3-δ} (BCY20) at 1100 °C [190], LSCF with BZY20 and BCY20 at 1100 °C [190]. The conclusions in [41] justified that LSCF had better chemical compatibility with LSGM and CeO₂-based electrolytes due to the formation of small amounts of impurity phases with LSGM9182 at 1300 °C and negligible interdiffusion with SDC at 1150 °C.

It should be noted that the use of LSM electrodes in contact with the BaCeO₃-based electrolytes is limited due to their active chemical interaction [191]. However, due to its high electronic conductivity and CTE compatibility, LSM can be successfully used as a collector for perspective layer electrodes for proton-conducting fuel cells operating in the IT range [192][193][194][195].

References

1. Erixno, O.; Rahim, N.A.; Ramadhani, F.; Adzman, N.N. Energy Management of Renewable Energy-Based Combined Heat and Power Systems: A Review. *Sustain. Energy Technol. Assess.* 2022, 51, 101944.
2. Iliev, I.K.; Filimonova, A.A.; Chichirov, A.A.; Chichirova, N.D.; Pechenkin, A.V.; Vinogradov, A.S. Theoretical and Experimental Studies of Combined Heat and Power Systems with SOFCs. *Energies* 2023, 16, 1898.
3. Lee, J.; Lin, K.-Y.A.; Jung, S.; Kwon, E.E. Hybrid Renewable Energy Systems Involving Thermochemical Conversion Process for Waste-to-Energy Strategy. *Chem. Eng. J.* 2023, 452, 139218.
4. He, V.; Gaffuri, M.; Van Herle, J.; Schiffmann, J. Readiness Evaluation of SOFC-MGT Hybrid Systems with Carbon Capture for Distributed Combined Heat and Power. *Energy Convers. Manag.* 2023, 278, 116728.
5. Wang, Y.; Cao, Q.; Liu, L.; Wu, Y.; Liu, H.; Gu, Z.; Zhu, C. A Review of Low and Zero Carbon Fuel Technologies: Achieving Ship Carbon Reduction Targets. *Sustain. Energy Technol. Assess.* 2022, 54, 102762.
6. Maestre, V.M.; Ortiz, A.; Ortiz, I. Challenges and Prospects of Renewable Hydrogen-Based Strategies for Full Decarbonization of Stationary Power Applications. *Renew. Sustain. Energy Rev.* 2021, 152, 111628.
7. Russo, M.A.; Carvalho, D.; Martins, N.; Monteiro, A. Forecasting the Inevitable: A Review on the Impacts of Climate Change on Renewable Energy Resources. *Sustain. Energy Technol. Assess.* 2022, 52, 102283.
8. Shen, M. Solid Oxide Fuel Cell-Lithium Battery Hybrid Power Generation System Energy Management: A Review. *Int. J. Hydrogen Energy* 2021, 46, 32974–32994.
9. Kumar, P.; Singh, O. A Review of Solid Oxide Fuel Cell Based Hybrid Cycles. *Int. J. Energy Res.* 2022, 46, 8560–8589.
10. Feng, Y.; Qu, J.; Zhu, Y.; Wu, B.; Wu, Y.; Xiao, Z.; Liu, J. Progress and Prospect of the Novel Integrated SOFC-ICE Hybrid Power System: System Design, Mass and Heat Integration, System Optimization and Techno-Economic Analysis. *Energy Convers. Manag.* 2023, 18, 100350.
11. Kasaeian, A.; Javidmehr, M.; Mirzaie, M.R.; Fereidooni, L. Integration of Solid Oxide Fuel Cells with Solar Energy Systems: A Review. *Appl. Therm. Eng.* 2023, 224, 120117.
12. Singh, M.; Zappa, D.; Comini, E. Solid Oxide Fuel Cell: Decade of Progress, Future Perspectives and Challenges. *Int. J. Hydrogen Energy* 2021, 46, 27643–27674.

13. Bilal Hanif, M.; Motola, M.; Qayyum, S.; Rauf, S.; Khalid, A.; Li, C.-J.; Li, C.-X. Recent Advancements, Doping Strategies and the Future Perspective of Perovskite-Based Solid Oxide Fuel Cells for Energy Conversion. *Chem. Eng. J.* 2022, 428, 132603.
14. Hu, S.; Li, J.; Zeng, Y.; Pu, J.; Chi, B. A Mini Review of the Recent Progress of Electrode Materials for Low-Temperature Solid Oxide Fuel Cells. *Phys. Chem. Chem. Phys.* 2023, 25, 5926–5941.
15. Tarutin, A.P.; Filonova, E.A.; Ricote, S.; Medvedev, D.A.; Shao, Z. Chemical Design of Oxygen Electrodes for Solid Oxide Electrochemical Cells: A Guide. *Sustain. Energy Technol. Assess.* 2023, 57, 103185.
16. Md Harashid, M.A.; Chen, R.S.; Ahmad, S.H.; Ismail, A.F.; Baharuddin, N.A. Recent Advances in Electrode Material for Symmetrical Solid Oxide Fuel Cells and Way Forward Sustainability Based on Local Mineral Resources. *Int. J. Energy Res.* 2022, 46, 22188–22221.
17. Tahir, N.N.M.; Baharuddin, N.A.; Samat, A.A.; Osman, N.; Somalu, M.R. A Review on Cathode Materials for Conventional and Proton-Conducting Solid Oxide Fuel Cells. *J. Alloys Compd.* 2022, 894, 162458.
18. Zhang, M.; Du, Z.; Zhang, Y.; Zhao, H. Progress of Perovskites as Electrodes for Symmetrical Solid Oxide Fuel Cells. *ACS Appl. Energy Mater.* 2022, 5, 13081–13095.
19. Pikalova, E.Y.; Kalinina, E.G.; Pikalova, N.S.; Filonova, E.A. High-Entropy Materials in SOFC Technology: Theoretical Foundations for Their Creation, Features of Synthesis, and Recent Achievements. *Materials* 2022, 15, 8783.
20. Skutina, L.; Filonova, E.; Medvedev, D.; Maignan, A. Undoped Sr₂MMoO₆ Double Perovskite Molybdates (M = Ni, Mg, Fe) as Promising Anode Materials for Solid Oxide Fuel Cells. *Materials* 2021, 14, 1715.
21. Curi, M.; da Silva, E.R.; de Furtado, J.G.M.; Ferraz, H.C.; Secchi, A.R. Anodes for SOFC: Review of Material Selection, Interface and Electrochemical Phenomena. *Quim. Nova* 2021, 44, 86–97.
22. Filonova, E.; Medvedev, D. Recent Progress in the Design, Characterisation and Application of LaAlO₃- and LaGaO₃-Based Solid Oxide Fuel Cell Electrolytes. *Nanomaterials* 2022, 12, 1991.
23. Kim, D.; Jeong, I.; Kim, K.J.; Bae, K.T.; Kim, D.; Koo, J.; Yu, H.; Lee, K.T. A Brief Review of Heterostructure Electrolytes for High-Performance Solid Oxide Fuel Cells at Reduced Temperatures. *J. Korean Ceram. Soc.* 2022, 59, 131–152.
24. Hanif, M.B.; Rauf, S.; Motola, M.; Babar, Z.U.D.; Li, C.-J.; Li, C.-X. Recent Progress of Perovskite-Based Electrolyte Materials for Solid Oxide Fuel Cells and Performance Optimizing Strategies for Energy Storage Applications. *Mater. Res. Bull.* 2022, 146, 111612.
25. Dey, S.; Chaudhary, S.; Parvatalu, D.; Mukhopadhyay, M.; Sharma, A.D.; Mukhopadhyay, J. Advancing Electrode Properties through Functionalization for Solid Oxide Cells Application: A

- Review. *Chem. Asian J.* 2023, 18, e202201222.
26. Kaur, P.; Singh, K. Review of Perovskite-Structure Related Cathode Materials for Solid Oxide Fuel Cells. *Ceram. Int.* 2020, 46, 5521–5535.
27. Jun, A.; Kim, J.; Shin, J.; Kim, G. Perovskite as a Cathode Material: A Review of Its Role in Solid-Oxide Fuel Cell Technology. *ChemElectroChem* 2016, 3, 511–530.
28. Klyndyuk, A.I.; Chizhova, E.A.; Kharytonau, D.S.; Medvedev, D.A. Layered oxygen-deficient double perovskites as promising cathode materials for solid oxide fuel cells. *Materials* 2022, 15, 141.
29. Vinoth Kumar, R.; Khandale, A.P. A Review on Recent Progress and Selection of Cobalt-Based Cathode Materials for Low Temperature-Solid Oxide Fuel Cells. *Renew. Sustain. Energy Rev.* 2022, 156, 111985.
30. Jiang, S.P. Development of Lanthanum Strontium Manganite Perovskite Cathode Materials of Solid Oxide Fuel Cells: A Review. *J. Mater. Sci.* 2008, 43, 6799–6833.
31. Carda, M.; Budáč, D.; Paidar, M.; Bouzek, K. Current Trends in the Description of Lanthanum Strontium Manganite Oxygen Electrode Reaction Mechanism in a High-Temperature Solid Oxide Cell. *Curr. Opin. Electrochem.* 2022, 31, 100852.
32. Oliveira, L.C.; Venâncio, R.; de Azevedo, P.V.; Anchieta, C.G.; Nepel, T.C.; Rodella, C.B.; Zanin, H.; Doubek, G. Reviewing Perovskite Oxide Sites Influence on Electrocatalytic Reactions for High Energy Density Devices. *J. Energy Chem.* 2023, 81, 1–19.
33. Jiang, S.P. Development of Lanthanum Strontium Cobalt Ferrite Perovskite Electrodes of Solid Oxide Fuel Cells—A Review. *Int. J. Hydrogen Energy* 2019, 44, 7448–7493.
34. Ndubuisi, A.; Abouali, S.; Singh, K.; Thangadurai, V. Recent Advances, Practical Challenges, and Perspectives of Intermediate Temperature Solid Oxide Fuel Cell Cathodes. *J. Mater. Chem. A* 2022, 10, 2196–2227.
35. Li, Z.; Li, M.; Zhu, Z. Perovskite Cathode Materials for Low-Temperature Solid Oxide Fuel Cells: Fundamentals to Optimization. *Electrochem. Energy Rev.* 2022, 5, 263–311.
36. Safian, S.D.; Abd Malek, N.I.; Jamil, Z.; Lee, S.-W.; Tseng, C.-J.; Osman, N. Study on the Surface Segregation of Mixed Ionic-Electronic Conductor Lanthanum-Based Perovskite Oxide $\text{La}_1 - x\text{Sr}_x\text{Co}_1 - y\text{Fe}_y\text{O}_3 - \delta$ Materials. *Int. J. Energy Res.* 2022, 46, 7101–7117.
37. Zarabi Golkhatmi, S.; Asghar, M.I.; Lund, P.D. A Review on Solid Oxide Fuel Cell Durability: Latest Progress, Mechanisms, and Study Tools. *Renew. Sustain. Energy Rev.* 2022, 161, 112339.
38. Connor, P.A.; Yue, X.; Savaniu, C.D.; Price, R.; Triantafyllou, G.; Cassidy, M.; Kerhervé, G.; Payne, D.J.; Maher, R.C.; Cohen, L.F.; et al. Tailoring SOFC Electrode Microstructures for Improved Performance. *Adv. Energy Mater.* 2018, 8, 1800120.

39. Celik, I.; Lee, S.; Abernathy, H.; Hackett, G. Performance Degradation Predictions Based on Microstructural Evolution Due to Grain Coarsening Effects in Solid Oxide Fuel Cell Electrodes. *J. Electrochem. Soc.* 2018, 165, F64–F74.
40. Geofrey Sahini, M.; Daud Lupyana, S. Perspective and Control of Cation Interdiffusion and Interface Reactions in Solid Oxide Fuel Cells (SOFCs). *Mater. Sci. Eng. B* 2023, 292, 116415.
41. Zhang, L.; Chen, G.; Dai, R.; Lv, X.; Yang, D.; Geng, S. A Review of the Chemical Compatibility between Oxide Electrodes and Electrolytes in Solid Oxide Fuel Cells. *J. Power Sources* 2021, 492, 229630.
42. Khan, M.Z.; Song, R.-H.; Mehran, M.T.; Lee, S.-B.; Lim, T.-H. Controlling Cation Migration and Inter-Diffusion across Cathode/Interlayer/Electrolyte Interfaces of Solid Oxide Fuel Cells: A Review. *Ceram. Int.* 2021, 47, 5839–5869.
43. Wang, F.; Kishimoto, H.; Ishiyama, T.; Develos-Bagarinao, K.; Yamaji, K.; Horita, T.; Yokokawa, H. A Review of Sulfur Poisoning of Solid Oxide Fuel Cell Cathode Materials for Solid Oxide Fuel Cells. *J. Power Sources* 2020, 478, 228763.
44. Wang, C.C.; O'Donnell, K.; Jian, L.; Jiang, S.P. Co-Deposition and Poisoning of Chromium and Sulfur Contaminants on La_{0.6}Sr_{0.4}Co_{0.2}Fe_{0.8}O₃ – δ Cathodes of Solid Oxide Fuel Cells. *J. Electrochem. Soc.* 2015, 162, F507–F512.
45. Wang, R.; Parent, L.R.; Gopalan, S.; Zhong, Y. Experimental and Computational Investigations on the SO₂ Poisoning of (La_{0.8}Sr_{0.2})_{0.95}MnO₃ Cathode Materials. *Adv. Powder Mater.* 2023, 2, 100062.
46. Horita, T. Chromium Poisoning for Prolonged Lifetime of Electrodes in Solid Oxide Fuel Cells—Review. *Ceram. Int.* 2021, 47, 7293–7306.
47. Zhou, L.; Mason, J.H.; Li, W.; Liu, X. Comprehensive Review of Chromium Deposition and Poisoning of Solid Oxide Fuel Cells (SOFCs) Cathode Materials. *Renew. Sustain. Energy Rev.* 2020, 134, 110320.
48. Wang, R.; Sun, Z.; Lu, Y.; Gopalan, S.; Basu, S.N.; Pal, U.B. Comparison of Chromium Poisoning between Lanthanum Strontium Manganite and Lanthanum Strontium Ferrite Composite Cathodes in Solid Oxide Fuel Cells. *J. Power Sources* 2020, 476, 228743.
49. Jiang, S.P.; Chen, X. Chromium Deposition and Poisoning of Cathodes of Solid Oxide Fuel Cells —A Review. *Int. J. Hydrogen Energy* 2014, 39, 505–531.
50. Li, Q.; Wang, X.; Jia, L.; Chi, B.; Pu, J.; Li, J. High Performance and Carbon-Deposition Resistance Metal-Supported Solid Oxide Fuel Cell with a Nickel–Manganese Spinel Modified Anode. *Mater. Today Energy* 2020, 17, 100473.

51. Girona, K.; Laurencin, J.; Fouletier, J.; Lefebvre-Joud, F. Carbon Deposition in CH₄/CO₂ Operated SOFC: Simulation and Experimentation Studies. *J. Power Sources* 2012, 210, 381–391.
52. Chen, K.; Jiang, S.P. Surface Segregation in Solid Oxide Cell Oxygen Electrodes: Phenomena, Mitigation Strategies and Electrochemical Properties. *Electrochem. Energy Rev.* 2020, 3, 730–765.
53. van Eck, N.J.; Waltman, L. Software Survey: VOSviewer, a Computer Program for Bibliometric Mapping. *Scientometrics* 2010, 84, 523–538.
54. Cherepanov, V.A.; Barkhatova, L.Y.; Voronin, V.I. Phase Equilibria in the La–Sr–Mn–O System. *J. Solid State Chem.* 1997, 134, 38–44.
55. Cherepanov, V.A.; Filonova, E.A.; Voronin, V.I.; Berger, I.F.; Barkhatova, L.Y. Phase Equilibria in the LaCoO₃–LaMnO₃–SrCoO_{2.5}–SrMnO₃ System. *Mater. Res. Bull.* 1999, 34, 1481–1489.
56. Filonova, E.A.; Demina, A.N.; Kleibaum, E.A.; Gavrilova, L.Y.; Petrov, A.N. Phase Equilibria in the System LaMnO₃+δ-SrMnO₃-LaFeO₃-SrFeO₃ – d. *Inorg. Mater.* 2006, 42, 443–447.
57. Yusenko, M.V.; Belyaev, V.D.; Demin, A.K.; Bronin, D.I.; Sobyanin, V.A.; Snytnikov, P.V. A Study of the Electrochemical Characteristics of Single-Chamber Solid Oxide Fuel Cells Based on Platinum and Strontium-Doped Lanthanum Manganite Electrodes and Fed with a Methane–Air Mixture. *Kinet. Catal.* 2022, 63, 117–122.
58. Mizusaki, J. Electronic Conductivity, Seebeck Coefficient, Defect and Electronic Structure of Nonstoichiometric La₁ – xSr_xMnO₃. *Solid State Ion.* 2000, 132, 167–180.
59. Mori, M.; Hiei, Y.; Sammes, N.M.; Tompsett, G.A. Thermal-Expansion Behaviors and Mechanisms for Ca- or Sr-Doped Lanthanum Manganite Perovskites under Oxidizing Atmospheres. *J. Electrochem. Soc.* 2000, 147, 1295.
60. Demina, A.N.; Polovnikova, K.P.; Filonova, E.A.; Petrov, A.N.; Demin, A.K.; Pikalova, E.Y. Thermal Expansion and Electrical Conductivity of La_{0.7}Sr_{0.3}Mn₁ – yCryO₃. *Inorg. Mater.* 2007, 43, 430–435.
61. Løken, A.; Ricote, S.; Wachowski, S. Thermal and Chemical Expansion in Proton Ceramic Electrolytes and Compatible Electrodes. *Crystals* 2018, 8, 365.
62. Tsvetkov, D.S.; Sereda, V.V.; Malyshkin, D.A.; Ivanov, I.L.; Zuev, A.Y. Chemical Lattice Strain in Nonstoichiometric Oxides: An Overview. *J. Mater. Chem. A* 2022, 10, 6351–6375.
63. Maiti, T.K.; Majhi, J.; Maiti, S.K.; Singh, J.; Dixit, P.; Rohilla, T.; Ghosh, S.; Bhushan, S.; Chattopadhyay, S. Zirconia- and Ceria-Based Electrolytes for Fuel Cell Applications: Critical Advancements toward Sustainable and Clean Energy Production. *Environ. Sci. Pollut. Res.* 2022, 29, 64489–64512.

64. Sameshima, S.; Kawaminami, M.; Hirata, Y. Thermal Expansion of Rare-Earth-Doped Ceria Ceramics. *J. Ceram. Soc. Jpn.* 2002, 110, 597–600.
65. Tsvinkinberg, V.A.; Tolkacheva, A.S.; Filonova, E.A.; Gyrdasova, O.I.; Pikalov, S.M.; Vorotnikov, V.A.; Vylkov, A.I.; Moskalenko, N.I.; Pikalova, E.Y. Structure, Thermal Expansion and Electrical Conductivity of $\text{La}_2 - x\text{Gd}_x\text{NiO}_4 + \delta$ ($0.0 \leq x \leq 0.6$) Cathode Materials for SOFC Applications. *J. Alloys Compd.* 2021, 853, 156728.
66. Lee, D.; Han, J.-H.; Chun, Y.; Song, R.-H.; Shin, D.R. Preparation and Characterization of Strontium and Magnesium Doped Lanthanum Gallates as the Electrolyte for IT-SOFC. *J. Power Sources* 2007, 166, 35–40.
67. Tietz, F. Thermal Expansion of SOFC Materials. *Ionics* 1999, 5, 129–139.
68. De Haart, L.G.J.; Vinke, I.C. Long-Term Operation of Planar Type SOFC Stacks. *ECS Trans.* 2011, 35, 187–194.
69. Kim-Lohsoontorn, P.; Brett, D.J.L.; Laosiripojana, N.; Kim, Y.-M.; Bae, J.-M. Performance of Solid Oxide Electrolysis Cells Based on Composite $\text{La}_0.8\text{Sr}_0.2\text{MnO}_3 - \delta$ —Yttria Stabilized Zirconia and $\text{Ba}_0.5\text{Sr}_0.5\text{Co}_0.8\text{Fe}_0.2\text{O}_3 - \delta$ Oxygen Electrodes. *Int. J. Hydrogen Energy* 2010, 35, 3958–3966.
70. De Souza, R.A.; Kilner, J.A.; Walker, J.F. A SIMS Study of Oxygen Tracer Diffusion and Surface Exchange in $\text{La}_0.8\text{Sr}_0.2\text{MnO}_3 + \delta$. *Mater. Lett.* 2000, 43, 43–52.
71. Tai, L. Structure and Electrical Properties of $\text{La}_1 - x\text{Sr}_x\text{Co}_1 - y\text{Fe}_y\text{O}_3$. Part 2. The System $\text{La}_1 - x\text{Sr}_x\text{Co}_0.2\text{Fe}_0.8\text{O}_3$. *Solid State Ion.* 1995, 76, 273–283.
72. Mineshige, A.; Izutsu, J.; Nakamura, M.; Nigaki, K.; Kobune, M.; Fujii, S.; Inaba, M.; Ogumi, Z.; Yao, T. Electrical Property, Crystal Structure and Oxygen Nonstoichiometry of $\text{La}_1 - x\text{Sr}_x\text{Co}_0.2\text{Fe}_0.8\text{O}_3 - \delta$. *Electrochemistry* 2000, 68, 515–518.
73. Teraoka, Y.; Zhang, H.M.; Okamoto, K.; Yamazoe, N. Mixed Ionic-Electronic Conductivity of $\text{La}_1 - x\text{Sr}_x\text{Co}_1 - y\text{Fe}_y\text{O}_3 - \delta$ Perovskite-Type Oxides. *Mater. Res. Bull.* 1988, 23, 51–58.
74. Petric, A. Evaluation of La–Sr–Co–Fe–O Perovskites for Solid Oxide Fuel Cells and Gas Separation Membranes. *Solid State Ion.* 2000, 135, 719–725.
75. Carter, S. Oxygen Transport in Selected Nonstoichiometric Perovskite-Structure Oxides. *Solid State Ion.* 1992, 53–56, 597–605.
76. Katsuki, M. High Temperature Properties of $\text{La}_0.6\text{Sr}_0.4\text{Co}_0.8\text{Fe}_0.2\text{O}_3 - \delta$ Oxygen Nonstoichiometry and Chemical Diffusion Constant. *Solid State Ion.* 2003, 156, 453–461.
77. Simner, S.P.; Anderson, M.D.; Engelhard, M.H.; Stevenson, J.W. Degradation Mechanisms of La–Sr–Co–Fe–O₃ SOFC Cathodes. *Electrochem. Solid-State Lett.* 2006, 9, A478.

78. Wang, H.; Barnett, S.A. Degradation Mechanisms of Porous La_{0.6}Sr_{0.4}Co_{0.2}Fe_{0.8}O₃ – δ Solid Oxide Fuel Cell Cathodes. *J. Electrochem. Soc.* 2018, 165, F564–F570.
79. Laurencin, J.; Hubert, M.; Sanchez, D.F.; Pylypko, S.; Morales, M.; Morata, A.; Morel, B.; Montinaro, D.; Lefebvre-Joud, F.; Siebert, E. Degradation Mechanism of La_{0.6}Sr_{0.4}Co_{0.2}Fe_{0.8}O₃ – δ/Gd_{0.1}Ce_{0.9}O₂ – δ Composite Electrode Operated under Solid Oxide Electrolysis and Fuel Cell Conditions. *Electrochim. Acta* 2017, 241, 459–476.
80. Zhao, L.; Drennan, J.; Kong, C.; Amarasinghe, S.; Jiang, S.P. Insight into Surface Segregation and Chromium Deposition on La_{0.6}Sr_{0.4}Co_{0.2}Fe_{0.8}O₃ – δ Cathodes of Solid Oxide Fuel Cells. *J. Mater. Chem. A* 2014, 2, 11114–11123.
81. Lee, W.; Han, J.W.; Chen, Y.; Cai, Z.; Yildiz, B. Cation Size Mismatch and Charge Interactions Drive Dopant Segregation at the Surfaces of Manganite Perovskites. *J. Am. Chem. Soc.* 2013, 135, 7909–7925.
82. He, S.; Jiang, S.P. Electrode/Electrolyte Interface and Interface Reactions of Solid Oxide Cells: Recent Development and Advances. *Prog. Nat. Sci.* 2021, 31, 341–372.
83. Stochniol, G.; Syskakis, E.; Naoumidis, A. Chemical Compatibility between Strontium-Doped Lanthanum Manganite and Yttria-Stabilized Zirconia. *J. Am. Ceram. Soc.* 1995, 78, 929–932.
84. Yokokawa, H.; Tu, H.; Iwanschitz, B.; Mai, A. Fundamental Mechanisms Limiting Solid Oxide Fuel Cell Durability. *J. Power Sources* 2008, 182, 400–412.
85. Kindermann, L. Chemical Compatibility of the LaFeO₃ Base Perovskites (La_{0.6}Sr_{0.4})ZFe_{0.8}M_{0.2}O₃ – δ (z = 1, 0.9; M = Cr, Mn, Co, Ni) with Yttria Stabilized Zirconia. *Solid State Ion.* 1996, 89, 215–220.
86. Hubert, M.; Laurencin, J.; Cloetens, P.; Mougin, J.; Ferreira Sanchez, D.; Pylypko, S.; Morales, M.; Morata, A.; Morel, B.; Montinaro, D.; et al. Solid Oxide Cell Degradation Operated in Fuel Cell and Electrolysis Modes: A Comparative Study on Ni Agglomeration and LSCF Destabilization. *ECS Trans.* 2017, 78, 3167–3177.
87. Kostogloudis, G. Chemical Reactivity of Perovskite Oxide SOFC Cathodes and Yttria Stabilized Zirconia. *Solid State Ion.* 2000, 135, 529–535.
88. Fan, B.; Yan, J.; Yan, X. The Ionic Conductivity, Thermal Expansion Behavior, and Chemical Compatibility of La_{0.54}Sr_{0.44}Co_{0.2}Fe_{0.8}O₃ – δ as SOFC Cathode Material. *Solid State Sci.* 2011, 13, 1835–1839.
89. Darvish, S.; Asadikiya, M.; Hu, B.; Singh, P.; Zhong, Y. Thermodynamic Prediction of the Effect of CO₂ to the Stability of (La_{0.8}Sr_{0.2})_{0.98}MnO₃±δ System. *Int. J. Hydrogen Energy* 2016, 41, 10239–10248.

90. Hu, B.; Mahapatra, M.K.; Keane, M.; Zhang, H.; Singh, P. Effect of CO₂ on the Stability of Strontium Doped Lanthanum Manganite Cathode. *J. Power Sources* 2014, 268, 404–413.
91. Zhao, Z.; Liu, L.; Zhang, X.; Wu, W.; Tu, B.; Ou, D.; Cheng, M. A Comparison on Effects of CO₂ on La_{0.8}Sr_{0.2}MnO_{3+δ} and La_{0.6}Sr_{0.4}CoO_{3 – δ} Cathodes. *J. Power Sources* 2013, 222, 542–553.
92. Darvish, S.; Gopalan, S.; Zhong, Y. Thermodynamic Stability Maps for the La_{0.6}Sr_{0.4}Co_{0.2}Fe_{0.8}O_{3±δ}–CO₂–O₂ System for Application in Solid Oxide Fuel Cells. *J. Power Sources* 2016, 336, 351–359.
93. Zhao, Z.; Liu, L.; Zhang, X.; Wu, W.; Tu, B.; Cui, D.; Ou, D.; Cheng, M. High- and Low-Temperature Behaviors of La_{0.6}Sr_{0.4}Co_{0.2}Fe_{0.8}O_{3 – δ} Cathode Operating under CO₂/H₂O-Containing Atmosphere. *Int. J. Hydrogen Energy* 2013, 38, 15361–15370.
94. Lai, S.Y.; Ding, D.; Liu, M.; Liu, M.; Alamgir, F.M. Operando and in Situ X-ray Spectroscopies of Degradation in La_{0.6}Sr_{0.4}Co_{0.2}Fe_{0.8}O_{3 – δ} Thin Film Cathodes in Fuel Cells. *ChemSusChem* 2014, 7, 3078–3087.
95. Liu, Y.L.; Hagen, A.; Barfod, R.; Chen, M.; Wang, H.J.; Poulsen, F.W.; Hendriksen, P.V. Microstructural Studies on Degradation of Interface between LSM–YSZ Cathode and YSZ Electrolyte in SOFCs. *Solid State Ion.* 2009, 180, 1298–1304.
96. Hu, B.; Mahapatra, M.K.; Singh, P. Performance Regeneration in Lanthanum Strontium Manganite Cathode during Exposure to H₂O and CO₂ Containing Ambient Air Atmospheres. *J. Ceram. Soc. Jpn.* 2015, 123, 199–204.
97. Xia, Z.; Zhao, D.; Zhou, Y.; Deng, Z.; Kupecki, J.; Fu, X.; Li, X. Control-Oriented Performance Prediction of Solid Oxide Electrolysis Cell and Durability Improvement through Retard Oxygen Electrode Delamination with Reverse Operation. *Energy Convers. Manag.* 2023, 277, 116596.
98. Wachsman, E.D.; Huang, Y.-L.; Pellegrinelli, C.; Taillon, J.A.; Salamanca-Riba, L.G. Towards a Fundamental Understanding of the Cathode Degradation Mechanisms. *ECS Trans.* 2014, 61, 47–56.
99. Wei, B.; Chen, K.; Zhao, L.; Lü, Z.; Jiang, S.P. Chromium Deposition and Poisoning at La_{0.6}Sr_{0.4}Co_{0.2}Fe_{0.8}O_{3 – δ} Oxygen Electrodes of Solid Oxide Electrolysis Cells. *Phys. Chem. Chem. Phys.* 2015, 17, 1601–1609.
100. Subotić, V.; Futamura, S.; Harrington, G.F.; Matsuda, J.; Natsukoshi, K.; Sasaki, K. Towards Understanding of Oxygen Electrode Processes during Solid Oxide Electrolysis Operation to Improve Simultaneous Fuel and Oxygen Generation. *J. Power Sources* 2021, 492, 229600.
101. He, S.; Saunders, M.; Chen, K.; Gao, H.; Suvorova, A.; Rickard, W.D.A.; Quadir, Z.; Cui, C.Q.; Jiang, S.P. A FIB-STEM Study of Strontium Segregation and Interface Formation of Directly

- Assembled La_{0.6}Sr_{0.4}Co_{0.2}Fe_{0.8}O₃ – δ Cathode on Y₂O₃-ZrO₂ Electrolyte of Solid Oxide Fuel Cells. *J. Electrochem. Soc.* 2018, 165, F417–F429.
102. Pellegrinelli, C.; Huang, Y.-L.; Wachsman, E.D. Effect of H₂O and CO₂ on LSCF–GDC Composite Cathodes. *ECS Trans.* 2019, 91, 665–680.
103. Xiong, C.; Qiu, P.; Zhang, W.; Pu, J. Influence of Practical Operating Temperature on the Cr Poisoning for LSCF-GDC Cathode. *Ceram. Int.* 2022, 48, 33999–34004.
104. Minh, N.Q. Development of Reversible Solid Oxide Fuel Cells (RSOFCs) and Stacks. *ECS Trans.* 2011, 35, 2897–2904.
105. Monaco, F.; Ferreira-Sanchez, D.; Hubert, M.; Morel, B.; Montinaro, D.; Grolimund, D.; Laurencin, J. Oxygen Electrode Degradation in Solid Oxide Cells Operating in Electrolysis and Fuel Cell Modes: LSCF Destabilization and Interdiffusion at the Electrode/Electrolyte Interface. *Int. J. Hydrogen Energy* 2021, 46, 31533–31549.
106. Lu, K.; Shen, F. Long Term Behaviors of La_{0.8}Sr_{0.2}MnO₃ and La_{0.6}Sr_{0.4}Co_{0.2}Fe_{0.8}O₃ as Cathodes for Solid Oxide Fuel Cells. *Int. J. Hydrogen Energy* 2014, 39, 7963–7971.
107. Türk, H.; Götsch, T.; Schmidt, F.; Hammud, A.; Ivanov, D.; (Bert) de Haart, L.G.J.; Vinke, I.C.; Eichel, R.; Schlögl, R.; Reuter, K.; et al. Sr Surface Enrichment in Solid Oxide Cells—Approaching the Limits of EDX Analysis by Multivariate Statistical Analysis and Simulations. *ChemCatChem* 2022, 14, e202200300.
108. Li, D.; Zhang, X.; Liang, C.; Jin, Y.; Fu, M.; Yuan, J.; Xiong, Y. Study on Durability of Novel Core-Shell-Structured La_{0.8}Sr_{0.2}Co_{0.2}Fe_{0.8}O₃ – δ@Gd_{0.2}Ce_{0.8}O_{1.9} Composite Materials for Solid Oxide Fuel Cell Cathodes. *Int. J. Hydrogen Energy* 2021, 46, 28221–28231.
109. Türk, H.; Schmidt, F.; Götsch, T.; Girgsdies, F.; Hammud, A.; Ivanov, D.; Vinke, I.C.; (Bert) de Haart, L.G.J.; Eichel, R.; Reuter, K.; et al. Complexions at the Electrolyte/Electrode Interface in Solid Oxide Cells. *Adv. Mater. Interfaces* 2021, 8, 2100967.
110. Cheng, K.; Xu, H.; Zhang, L.; Du, Y.; Zhou, J.; Tang, S.; Chen, M. Numerical Simulation of the SrZrO₃ Formation in Solid Oxide Fuel Cells. *J. Electron. Mater.* 2019, 48, 5510–5515.
111. Jacobs, R.; Liu, J.; Na, B.T.; Guan, B.; Yang, T.; Lee, S.; Hackett, G.; Kalapos, T.; Abernathy, H.; Morgan, D. Unconventional Highly Active and Stable Oxygen Reduction Catalysts Informed by Computational Design Strategies. *Adv. Energy Mater.* 2022, 12, 2201203.
112. Han, H.; Hu, X.; Zhang, B.; Zhang, S.; Zhang, Y.; Xia, C. Method to Determine the Oxygen Reduction Reaction Kinetics via Porous Dual-Phase Composites Based on Electrical Conductivity Relaxation. *J. Mater. Chem. A* 2023, 11, 2460–2471.
113. Yan, Z.; He, A.; Hara, S.; Shikazono, N. Design and Optimization of Functionally Graded Electrodes for Solid Oxide Fuel Cells (SOFCs) by Mesoscale Modeling. *Int. J. Hydrogen Energy*

2022, 47, 16610–16625.

114. Padinjarethil, A.K.; Bianchi, F.R.; Bosio, B.; Hagen, A. Electrochemical Characterization and Modelling of Anode and Electrolyte Supported Solid Oxide Fuel Cells. *Front. Energy Res.* 2021, 9, 668964.
115. Bliem, R.; Kim, D.; Wang, J.; Crumlin, E.J.; Yildiz, B. Hf Deposition Stabilizes the Surface Chemistry of Perovskite Manganite Oxide. *J. Phys. Chem. C* 2021, 125, 3346–3354.
116. Zeng, D.; Xu, K.; Zhu, F.; Chen, Y. Enhancing the Oxygen Reduction Reaction Activity and Durability of a Solid Oxide Fuel Cell Cathode by Surface Modification of a Hybrid Coating. *Int. J. Hydrogen Energy* 2023, 48, 23992–24001.
117. Li, J.; Zhou, X.; Wu, C.; Zhao, L.; Dong, B.; Wang, S.; Chi, B. Self-Stabilized Hybrid Cathode for Solid Oxide Fuel Cell: A-Site Deficient Perovskite Coating as Solid Solution for Strontium Diffusion. *Chem. Eng. J.* 2022, 438, 135446.
118. Zhang, X.; Jin, Y.; Jiang, Y.; Zong, X.; Li, Y.; Xiong, Y. Enhancing Chromium Poisoning Tolerance of La_{0.8}Sr_{0.2}Co_{0.2}Fe_{0.8}O₃ – δ Cathode by Ce_{0.8}Gd_{0.2}O_{1.9} – δ Coating. *J. Power Sources* 2022, 547, 231996.
119. Pei, K.; Zhou, Y.; Ding, Y.; Xu, K.; Zhang, H.; Yuan, W.; Sasaki, K.; Choi, Y.; Liu, M.; Chen, Y. An Improved Oxygen Reduction Reaction Activity and CO₂-Tolerance of La_{0.6}Sr_{0.4}Co_{0.2}Fe_{0.8}O₃ – δ Achieved by a Surface Modification with Barium Cobaltite Coatings. *J. Power Sources* 2021, 514, 230573.
120. Pei, K.; Zhou, Y.; Xu, K.; He, Z.; Chen, Y.; Zhang, W.; Yoo, S.; Zhao, B.; Yuan, W.; Liu, M.; et al. Enhanced Cr-Tolerance of an SOFC Cathode by an Efficient Electro-Catalyst Coating. *Nano Energy* 2020, 72, 104704.
121. Ishfaq, H.A.; Khan, M.Z.; Shirke, Y.M.; Qamar, S.; Hussain, A.; Mehran, M.T.; Song, R.-H.; Saleem, M. A Heuristic Approach to Boost the Performance and Cr Poisoning Tolerance of Solid Oxide Fuel Cell Cathode by Robust Multi-Doped Ceria Coating. *Appl. Catal. B Environ.* 2023, 323, 122178.
122. Chen, Y.; Hinerman, A.; Liang, L.; Gerdes, K.; Navia, S.P.; Prucz, J.; Song, X. Conformal Coating of Cobalt Oxide on Solid Oxide Fuel Cell Cathode and Resultant Continuously Increased Oxygen Reduction Reaction Kinetics upon Operation. *J. Power Sources* 2018, 405, 45–50.
123. Niu, Y.; Zhou, Y.; Zhang, W.; Zhang, Y.; Evans, C.; Luo, Z.; Kane, N.; Ding, Y.; Chen, Y.; Guo, X.; et al. Highly Active and Durable Air Electrodes for Reversible Protonic Ceramic Electrochemical Cells Enabled by an Efficient Bifunctional Catalyst. *Adv. Energy Mater.* 2022, 12, 2103783.
124. Zhang, X.; Jin, Y.; Li, D.; Zong, X.; Xiong, Y. Effects of Gd_{0.8}Ce_{0.2}O_{1.9} – δ Coating with Different Thickness on Electrochemical Performance and Long-Term Stability of La_{0.8}Sr_{0.2}Co_{0.2}Fe_{0.8}O₃ – δ Cathode in SOFCs. *Int. J. Hydrogen Energy* 2022, 47, 4100–4108.

125. Chen, Y.; Paredes-Navia, S.A.; Romo-De-La-Cruz, C.-O.; Liang, L.; Fernandes, A.; Hinerman, A.; Prucz, J.; Williams, M.; Song, X. Coating Internal Surface of Porous Electrode for Decreasing the Ohmic Resistance and Shifting Oxygen Reduction Reaction Pathways in Solid Oxide Fuel Cells. *J. Power Sources* 2021, 499, 229854.
126. Niu, Y.; Zhou, Y.; Lv, W.; Chen, Y.; Zhang, Y.; Zhang, W.; Luo, Z.; Kane, N.; Ding, Y.; Soule, L.; et al. Enhancing Oxygen Reduction Activity and Cr Tolerance of Solid Oxide Fuel Cell Cathodes by a Multiphase Catalyst Coating. *Adv. Funct. Mater.* 2021, 31, 2100034.
127. Yokokawa, H.; Horita, T. Cathodes. In High Temperature and Solid Oxide Fuel Cells; Elsevier: Amsterdam, The Netherlands, 2003; pp. 119–147. ISBN 978-1-85617-387-2.
128. Filonova, E.A.; Gilev, A.R.; Skutina, L.S.; Vylkov, A.I.; Kuznetsov, D.K.; Shur, V.Y. Double $\text{Sr}_2\text{Ni}_1 - x\text{Mg}_x\text{Mo}_6$ Perovskites ($x = 0, 0.25$) as Perspective Anode Materials for LaGaO_3 -Based Solid Oxide Fuel Cells. *Solid State Ion.* 2018, 314, 112–118.
129. Wu, Y.; Sang, J.; Liu, Z.; Fan, H.; Cao, B.; Wang, Q.; Yang, J.; Guan, W.; Liu, X.; Wang, J. Enhancing the Performance and Stability of Solid Oxide Fuel Cells by Adopting Samarium-Doped Ceria Buffer Layer. *Ceram. Int.* 2023, 49, 20290–20297.
130. Yang, Q.; Wang, Y.; Tian, D.; Wu, H.; Ding, Y.; Lu, X.; Chen, Y.; Lin, B. Enhancing Performance and Stability of Symmetrical Solid Oxide Fuel Cells via Quasi-Symmetrical Ceria-Based Buffer Layers. *Ceram. Int.* 2022, 48, 27509–27515.
131. Zhang, Y.; Niu, B.; Hao, X.; Wang, Y.; Liu, J.; Jiang, P.; He, T. Layered Oxygen-Deficient Double Perovskite $\text{GdBaFe}_2\text{O}_{5+\delta}$ as Electrode Material for Symmetrical Solid-Oxide Fuel Cells. *Electrochim. Acta* 2021, 370, 137807.
132. Niemczyk, A.; Zheng, K.; Cichy, K.; Berent, K.; Küster, K.; Starke, U.; Poudel, B.; Dabrowski, B.; Świerczek, K. High Cu Content $\text{LaNi}_{1-x}\text{Cu}_x\text{O}_3 - \delta$ Perovskites as Candidate Air Electrode Materials for Reversible Solid Oxide Cells. *Int. J. Hydrogen Energy* 2020, 45, 29449–29464.
133. Yang, X.; Li, R.; Yang, Y.; Wen, G.; Tian, D.; Lu, X.; Ding, Y.; Chen, Y.; Lin, B. Improving Stability and Electrochemical Performance of $\text{Ba}_0.5\text{Sr}_0.5\text{Co}_0.2\text{Fe}_0.8\text{O}_3 - \delta$ Electrode for Symmetrical Solid Oxide Fuel Cells by Mo Doping. *J. Alloys Compd.* 2020, 831, 154711.
134. Huang, K.; Wan, J.; Goodenough, J.B. Oxide-Ion Conducting Ceramics for Solid Oxide Fuel Cells. *J. Mater. Sci.* 2001, 36, 1093–1098.
135. Yun, J.W.; Yoon, S.P.; Park, S.; Han, J.; Nam, S.W.; Lim, T.-H.; Kim, J.-S. Modifying the Cathodes of Intermediate-Temperature Solid Oxide Fuel Cells with a $\text{Ce}_0.8\text{Sm}_0.2\text{O}_2$ Sol–Gel Coating. *Int. J. Hydrogen Energy* 2009, 34, 9213–9219.
136. Hanifi, A.R.; Paulson, S.; Torabi, A.; Shinbine, A.; Tucker, M.C.; Birss, V.; Etsell, T.H.; Sarkar, P. Slip-Cast and Hot-Solution Infiltrated Porous Yttria Stabilized Zirconia (YSZ) Supported Tubular Fuel Cells. *J. Power Sources* 2014, 266, 121–131.

137. Hwang, S.; Lee, J.; Kang, G.; Choi, M.; Kim, S.J.; Lee, W.; Byun, D. A Hydrogel-Assisted GDC Chemical Diffusion Barrier for Durable Solid Oxide Fuel Cells. *J. Mater. Chem. A* 2021, 9, 11683–11690.
138. Liu, Y.; Tian, Y.; Wang, Y.; Li, Y.; Pu, J.; Ciucci, F.; Chi, B. Nano Film Pr₂Ni0.8Cu0.2O_{4+δ} Decorated La_{0.6}Sr_{0.4}Co_{0.2}Fe_{0.8}O₃ – δ Oxygen Electrode for Highly Efficient and Stable Reversible Solid Oxide Cells. *Electrochim. Acta* 2022, 430, 141032.
139. Wang, Y.; Xu, N.; Dogdibegovic, E.; Su, T.; Brocato, A.D.; Zhou, X.-D. Role of Mixed Conducting Pr_{0.1}Gd_{0.1}Ce_{0.8}O_{1.9} – δ Barrier Layer on the Promotion of SOFC Performance. *Int. J. Hydrogen Energy* 2022, 47, 1917–1924.
140. Park, J.H.; Jung, C.H.; Kim, K.J.; Kim, D.; Shin, H.R.; Hong, J.-E.; Lee, K.T. Enhancing Bifunctional Electrocatalytic Activities of Oxygen Electrodes via Incorporating Highly Conductive Sm³⁺ and Nd³⁺ Double-Doped Ceria for Reversible Solid Oxide Cells. *ACS Appl. Mater. Interfaces* 2021, 13, 2496–2506.
141. Park, J.H.; Han, S.M.; Kim, B.-K.; Lee, J.-H.; Yoon, K.J.; Kim, H.; Ji, H.-I.; Son, J.-W. Sintered Powder-Base Cathode over Vacuum-Deposited Thin-Film Electrolyte of Low-Temperature Solid Oxide Fuel Cell: Performance and Stability. *Electrochim. Acta* 2019, 296, 1055–1063.
142. Choi, H.-J.; Na, Y.-H.; Kwak, M.; Kim, T.W.; Seo, D.-W.; Woo, S.-K.; Kim, S.-D. Development of Solid Oxide Cells by Co-Sintering of GDC Diffusion Barriers with LSCF Air Electrode. *Ceram. Int.* 2017, 43, 13653–13660.
143. Yoo, Y.-S.; Jeon, S.-Y.; Park, M.-A.; Lee, J.; Lee, Y. Electrochemical Performance of Solid Oxide Electrolysis Cells with LSCF6428–SDC/SDC Electrode for H₂O/CO₂ High Temperature Co-Electrolysis. *ECS Trans.* 2017, 78, 3123–3128.
144. Zhang, G.; Zheng, G.; Huang, Z.; Bao, X.; Shi, C.; Yang, X.; Zhou, J.; Chen, T.; Wang, S. The Effect of Fe₂O₃ Sintering Aid on Gd_{0.1}Ce_{0.9}O_{1.95} Diffusion Barrier Layer and Solid Oxide Fuel Cell Performance. *Int. J. Hydrogen Energy* 2023, 48, 21908–21919.
145. Budiman, R.A.; Yamaguchi, T.; Ishiyama, T.; Develos-Bagarinao, K.; Yamaji, K.; Kishimoto, H. Interlayer Modification for High-Performance and Stable Solid Oxide Electrolysis Cell. *Mater. Lett.* 2022, 309, 131419.
146. Wu, P.; Tian, Y.; Lü, Z.; Zhang, X.; Ding, L. Electrochemical Performance of La_{0.65}Sr_{0.35}MnO₃ Oxygen Electrode with Alternately Infiltrated Sm_{0.5}Sr_{0.5}CoO₃ – δ and Sm_{0.2}Ce_{0.8}O_{1.9} Nanoparticles for Reversible Solid Oxide Cells. *Int. J. Hydrogen Energy* 2022, 47, 747–760.
147. Yaroslavtsev, I.Y.; Kuzin, B.L.; Bronin, D.I.; Bogdanovich, N.M. Polarization Characteristics of Composite Electrodes in Electrochemical Cells with Solid Electrolytes Based on CeO₂ and LaGaO₃. *Russ. J. Electrochem.* 2005, 41, 527–531.

148. Mosiałek, M.; Zimowska, M.; Kharytonau, D.; Komenda, A.; Górska, M.; Krzan, M. Improvement of La_{0.8}Sr_{0.2}MnO₃ – δ Cathode Material for Solid Oxide Fuel Cells by Addition of YFe_{0.5}Co_{0.5}O₃. *Materials* 2022, 15, 642.
149. Bogdanovich, N.M.; Bronin, D.I.; Vdovin, G.K.; Yaroslavtsev, I.Y.; Kuzin, B.L. Effect of Bi_{0.75}Y_{0.25}O_{1.5} Electrolyte Additive in Collector Layer to Properties of Bilayer Composite Cathodes of Solid Oxide Fuel Cells Based on La(Sr)MnO₃ and La(Sr)Fe(Co)O₃ Compounds. *Russ. J. Electrochem.* 2009, 45, 456–464.
150. Perry Murray, E. (La,Sr)MnO₃–(Ce,Gd)O₂ – x Composite Cathodes for Solid Oxide Fuel Cells. *Solid State Ion.* 2001, 143, 265–273.
151. Chen, G.; Gao, Y.; Luo, Y.; Guo, R. Effect of A Site Deficiency of LSM Cathode on the Electrochemical Performance of SOFCs with Stabilized Zirconia Electrolyte. *Ceram. Int.* 2017, 43, 1304–1309.
152. Sun, K.; Yu, Z.; Ni, Q.; Li, Y.; Xu, D.; Gu, Y.; Zheng, Y.; Chen, H.; Ge, L.; Guo, L. Highly Durable Sr-Doped LaMnO₃-Based Cathode Modified with Pr₆O₁₁ Nano-Catalyst for Protonic Ceramic Fuel Cells Based on Y-Doped BaZrO₃ Electrolyte. *J. Eur. Ceram. Soc.* 2022, 42, 4266–4274.
153. Cao, X.G.; Jiang, S.P. Identification of Oxygen Reduction Processes at (La,Sr)MnO₃ Electrode/La_{9.5}Si₆O_{26.25} Apatite Electrolyte Interface of Solid Oxide Fuel Cells. *Int. J. Hydrogen Energy* 2013, 38, 2421–2431.
154. Strandbakke, R.; Dyrlie, O.; Hage, F.S.; Norby, T. Reaction Kinetics of Protons and Oxide Ions in LSM/Lanthanum Tungstate Cathodes with Pt Nanoparticle Activation. *J. Electrochem. Soc.* 2016, 163, F507–F515.
155. Shen, F.; Wang, R.; Tucker, M.C. Long Term Durability Test and Post Mortem for Metal-Supported Solid Oxide Electrolysis Cells. *J. Power Sources* 2020, 474, 228618.
156. Mater, A.; Othmani, A.; Boukhachem, A.; Madani, A. Cathode Performance Study of La_{0.6}Sr_{0.4}Co_{0.8}Fe_{0.2}O₃ – δ with Various Electrolyte-Doped Ceria Ce_{0.8}Sm_{0.17}Ln_{0.03}O_{1.9} for IT-Solid Oxide Fuel Cell. *J. Electron. Mater.* 2020, 49, 4123–4133.
157. Yang, C.; Cheng, J.G.; He, H.G.; Gao, J.F. Ni/SDC Materials for Solid Oxide Fuel Cell Anode Applications by the Glycine-Nitrate Method. *Key Eng. Mater.* 2010, 434–435, 731–734.
158. Ahuja, A.; Gautam, M.; Sinha, A.; Sharma, J.; Patro, P.K.; Venkatasubramanian, A. Effect of Processing Route on the Properties of LSCF-Based Composite Cathode for IT-SOFC. *Bull. Mater. Sci.* 2020, 43, 129.
159. He, A.; Onishi, J.; Shikazono, N. Optimization of Electrode-Electrolyte Interface Structure for Solid Oxide Fuel Cell Cathode. *J. Power Sources* 2020, 449, 227565.

160. Loureiro, F.J.A.; Macedo, D.A.; Nascimento, R.M.; Cesário, M.R.; Grilo, J.P.F.; Yaremchenko, A.A.; Fagg, D.P. Cathodic Polarisation of Composite LSCF-SDC IT-SOFC Electrode Synthesised by One-Step Microwave Self-Assisted Combustion. *J. Eur. Ceram. Soc.* 2019, 39, 1846–1853.
161. Wei, F.; Wang, L.; Luo, L.; Cheng, L.; Xu, X. One-Pot Impregnation to Construct Nanoparticles Loaded Scaffold Cathode with Enhanced Oxygen Reduction Performance for LT-SOFCs. *J. Alloys Compd.* 2023, 941, 168981.
162. Sun, Y.; He, S.; Saunders, M.; Chen, K.; Shao, Z.; Jiang, S.P. A Comparative Study of Surface Segregation and Interface of La_{0.6}Sr_{0.4}Co_{0.2}Fe_{0.8}O₃ – δ Electrode on GDC and YSZ Electrolytes of Solid Oxide Fuel Cells. *Int. J. Hydrogen Energy* 2021, 46, 2606–2616.
163. Abarzua, G.; Udayabhaskar, R.; Mangalaraja, R.V.; Durango-Petro, J.; Usuba, J.; Flies, H. A Feasible Strategy for Tailoring Stable Spray-Coated Electrolyte Layer in Micro-Tubular Solid Oxide Fuel Cells. *Int. J. Appl. Ceram. Technol.* 2022, 19, 1389–1396.
164. Samreen, A.; Galvez-Sanchez, M.; Steinberger-Wilckens, R.; Arifin, N.A.; Saher, S.; Ali, S.; Qamar, A. Electrochemical Performance of Novel NGCO–LSCF Composite Cathode for Intermediate Temperature Solid Oxide Fuel Cells. *Int. J. Hydrogen Energy* 2020, 45, 21714–21721.
165. Hong, T.; Lee, S.; Ohodnicki, P.; Brinkman, K. A Highly Scalable Spray Coating Technique for Electrode Infiltration: Barium Carbonate Infiltrated La_{0.6}Sr_{0.4}Co_{0.2}Fe_{0.8}O₃ – δ Perovskite Structured Electrocatalyst with Demonstrated Long Term Durability. *Int. J. Hydrogen Energy* 2017, 42, 24978–24988.
166. Tsuji, Y.; Amezawa, K.; Nakao, T.; Ina, T.; Kawada, T.; Yamamoto, K.; Uchimoto, Y.; Orikasa, Y. Investigation of Cathodic Reaction Mechanism in Solid Oxide Fuel Cells by Operando X-ray Absorption Spectroscopy. *Electrochemistry* 2020, 88, 560–565.
167. Chen, X.; Sun, X.; Zhou, J.; Zhou, D.; Zhu, X.; Meng, J. Effects of CoO and Bi₂O₃ Single/Dual Sintering Aids Doping on Structure and Properties of Ce_{0.8}Nd_{0.2}O_{1.9}. *Ceram. Int.* 2020, 46, 22727–22732.
168. Wang, Y.-P.; Liu, S.-H.; Zhang, H.-Y.; Li, C.-X.; Zhang, S.-L.; Yang, G.-J.; Li, C.-J. Structured La_{0.6}Sr_{0.4}Co_{0.2}Fe_{0.8}O₃ – δ Cathode with Large-Scale Vertical Cracks by Atmospheric Laminar Plasma Spraying for IT-SOFCs. *J. Alloys Compd.* 2020, 825, 153865.
169. Wang, J.; Yang, Z.; Yang, K.; Peng, S. Kinetics of Oxygen Reaction in Porous La_{0.6}Sr_{0.4}Co_{0.2}Fe_{0.8}O₃ – δ-Ce_{0.8}Gd_{0.2}O_{1.9} Composite Electrodes for Solid Oxide Cells. *Int. J. Hydrogen Energy* 2021, 46, 25608–25619.
170. Khaerudini, D.S.; Guan, G.; Zhang, P.; Hao, X.; Wang, Z.; Xue, C.; Kasai, Y.; Abudula, A. Performance Assessment of Bi_{0.3}Sr_{0.7}Co_{0.3}Fe_{0.7}O₃ – δ–LSCF Composite as Cathode for

- Intermediate-Temperature Solid Oxide Fuel Cells with La_{0.8}Sr_{0.2}Ga_{0.8}Mg_{0.2}O₃ – δ Electrolyte. *J. Power Sources* 2015, 298, 269–279.
171. Zhang, S.-L.; Shang, Y.-B.; Li, C.-X.; Li, C.-J. Vacuum Cold Sprayed Nanostructured La_{0.6}Sr_{0.4}Co_{0.2}Fe_{0.8}O₃ – δ as a High-Performance Cathode for Porous Metal-Supported Solid Oxide Fuel Cells Operating below 600 °C. *Mater. Today Energy* 2021, 21, 100815.
172. Wang, S.-F.; Lu, H.-C.; Hsu, Y.-F.; Jasinski, P. High-Performance Anode-Supported Solid Oxide Fuel Cells with Co-Fired Sm_{0.2}Ce_{0.8}O₂ – δ/La_{0.8}Sr_{0.2}Ga_{0.8}Mg_{0.2}O₃ – δ/Sm_{0.2}Ce_{0.8}O₂ – δ Sandwiched Electrolyte. *Int. J. Hydrogen Energy* 2022, 47, 5429–5438.
173. Lei, L.; Tao, Z.; Hong, T.; Wang, X.; Chen, F. A Highly Active Hybrid Catalyst Modified (La_{0.60}Sr_{0.40})_{0.95}Co_{0.20}Fe_{0.80}O₃ – δ Cathode for Proton Conducting Solid Oxide Fuel Cells. *J. Power Sources* 2018, 389, 1–7.
174. Di Bartolomeo, E.; Zunic, M.; Chevallier, L.; D'Epifanio, A.; Licoccia, S.; Traversa, E. Fabrication of Proton Conducting Solid Oxide Fuel Cells by Using Electrophoretic Deposition. *ECS Trans.* 2009, 25, 577–584.
175. Watanabe, K.; Yamaguchi, Y.; Nomura, K.; Sumi, H.; Mori, M.; Mizutani, Y.; Shimada, H. Effect of Cobalt Content on Electrochemical Performance for La_{0.6}Sr_{0.4}CoxFe_{1-x}O₃ – δ and BaZr_{0.8}Yb_{0.2}O₃ – δ Composite Cathodes in Protonic Ceramic Fuel Cells. *Ceram. Int.* 2023, 49, 21085–21090.
176. Vafaeenezhad, S.; Sandhu, N.K.; Hanifi, A.R.; Etsell, T.H.; Sarkar, P. Development of Proton Conducting Fuel Cells Using Nickel Metal Support. *J. Power Sources* 2019, 435, 226763.
177. Zhang, Q.; Hou, Y.; Chen, L.; Wang, L.; Chou, K. Enhancement of Electrochemical Performance for Proton Conductive Solid Oxide Fuel Cell by 30%GDC-LSCF Cathode. *Ceram. Int.* 2022, 48, 17816–17827.
178. Chen, X.; Zhang, H.; Li, Y.; Xing, J.; Zhang, Z.; Ding, X.; Zhang, B.; Zhou, J.; Wang, S. Fabrication and Performance of Anode-Supported Proton Conducting Solid Oxide Fuel Cells Based on BaZr_{0.1}Ce_{0.7}Y_{0.1}Yb_{0.1}O₃ – δ Electrolyte by Multi-Layer Aqueous-Based Co-Tape Casting. *J. Power Sources* 2021, 506, 229922.
179. Shimada, H.; Yamaguchi, Y.; Sumi, H.; Mizutani, Y. Performance Comparison of Perovskite Composite Cathodes with BaZr_{0.1}Ce_{0.7}Y_{0.1}Yb_{0.1}O₃ – δ in Anode-Supported Protonic Ceramic Fuel Cells. *J. Electrochem. Soc.* 2020, 167, 124506.
180. Gao, J.; Meng, Y.; Lee, S.; Tong, J.; Brinkman, K.S. Effect of Infiltration of Barium Carbonate Nanoparticles on the Electrochemical Performance of La_{0.6}Sr_{0.4}Co_{0.2}Fe_{0.8}O₃ – δ Cathodes for Protonic Ceramic Fuel Cells. *JOM* 2019, 71, 90–95.
181. Lai, Y.-W.; Lee, K.-R.; Yang, S.-Y.; Tseng, C.-J.; Jang, S.-C.; Tsao, I.-Y.; Chen, S.; Lee, S.-W. Production of La_{0.6}Sr_{0.4}Co_{0.2}Fe_{0.8}O₃ – δ Cathode with Graded Porosity for Improving Proton-

- Conducting Solid Oxide Fuel Cells. *Ceram. Int.* 2019, 45, 22479–22485.
182. Fan, Y.; Xi, X.; Li, J.; Wang, Q.; Xiang, K.; Medvedev, D.; Luo, J.-L.; Fu, X.-Z. Barium-Doped $\text{Sr}_2\text{Fe}_{1.5}\text{Mo}_{0.5}\text{O}_6 - \delta$ Perovskite Anode Materials for Protonic Ceramic Fuel Cells for Ethane Conversion. *J. Am. Ceram. Soc.* 2022, 105, 3613–3624.
183. Gao, Y.; Yang, Y.; Lin, X.; Fu, M.; Hu, W.; Tong, H.; Tao, Z. Investigation and Study of Three Different Composite Cathodes for Proton-Conducting Solid Oxide Fuel Cells. *Sep. Purif. Technol.* 2022, 300, 121890.
184. Lee, H.; Lee, S.; Lee, T.; Park, S.; Shin, D. Long Term Stability of Porosity Gradient Composite Cathode Controlled by Electro-Static Slurry Spray Deposition. *Int. J. Hydrogen Energy* 2017, 42, 3748–3752.
185. Hanif, M.B.; Rauf, S.; Abadeen, Z.U.; Khan, K.; Tayyab, Z.; Qayyum, S.; Mosiątek, M.; Shao, Z.; Li, C.-X.; Motola, M. Proton-Conducting Solid Oxide Electrolysis Cells: Relationship of Composition-Structure-Property, Their Challenges, and Prospects. *Matter* 2023, 6, 1782–1830.
186. Zayas-Rey, M.J.; Dos Santos-Gómez, L.; Porras-Vázquez, J.M.; Losilla, E.R.; Marrero-López, D. Evaluation of Lanthanum Tungstates as Electrolytes for Proton Conductors Solid Oxide Fuel Cells. *J. Power Sources* 2015, 294, 483–493.
187. Marrero-López, D.; Martín-Sedeño, M.C.; Peña-Martínez, J.; Ruiz-Morales, J.C.; Núñez, P.; Aranda, M.A.G.; Ramos-Barrado, J.R. Evaluation of Apatite Silicates as Solid Oxide Fuel Cell Electrolytes. *J. Power Sources* 2010, 195, 2496–2506.
188. Nesaraj, A.S.; Kumar, M.; Arul Raj, I.; Radhakrishna, I.; Pattabiraman, R. Investigations on Chemical Interactions between Alternate Cathodes and Lanthanum Gallate Electrolyte for Intermediate Temperature Solid Oxide Fuel Cell (ITSOFC). *J. Iran. Chem. Soc.* 2007, 4, 89–106.
189. Giannici, F.; Chiara, A.; Canu, G.; Longo, A.; Martorana, A. Interface Solid-State Reactions in $\text{La}_{0.8}\text{Sr}_{0.2}\text{MnO}_3/\text{Ce}_{0.8}\text{Sm}_{0.2}\text{O}_2$ and $\text{La}_{0.8}\text{Sr}_{0.2}\text{MnO}_3/\text{BaCe}_{0.9}\text{Y}_{0.1}\text{O}_3$ Disclosed by X-ray Microspectroscopy. *ACS Appl. Energy Mater.* 2019, 2, 3204–3210.
190. Lyagaeva, J.; Medvedev, D.; Pikalova, E.; Plaksin, S.; Brouzgou, A.; Demin, A.; Tsiakaras, P. A Detailed Analysis of Thermal and Chemical Compatibility of Cathode Materials Suitable for $\text{BaCe}_{0.8}\text{Y}_{0.2}\text{O}_3 - \delta$ and $\text{BaZr}_{0.8}\text{Y}_{0.2}\text{O}_3 - \delta$ Proton Electrolytes for Solid Oxide Fuel Cell Application. *Int. J. Hydrogen Energy* 2017, 42, 1715–1723.
191. Pikalova, E.; Bogdanovich, N.; Kolchugin, A.; Brouzgou, A.; Bronin, D.; Plaksin, S.V.; Khasanov, A.; Tsiakaras, P. Effect of Nature of the Ceramic Component of the Composite Electrodes Based on $\text{La}_{1.7}\text{Ca}(\text{Sr})_{0.3}\text{NiO}_4 + \delta$ on Their Electrochemical Performance. *ECS Trans.* 2015, 68, 809–815.
192. Antonova, E.P.; Kolchugin, A.A.; Pikalova, E.Y.; Medvedev, D.A.; Bogdanovich, N.M. Development of Electrochemically Active Electrodes for $\text{BaCe}_{0.89}\text{Gd}_{0.1}\text{Cu}_{0.01}\text{O}_3 - \delta$ Proton Conducting

Electrolyte. Solid State Ion. 2017, 306, 55–61.

193. Pikalova, E.Y.; Kolchugin, A.A. The Influence of the Substituting Element ($M = Ca, Sr, Ba$) in $La1.7M0.3NiO4+\delta$ on the Electrochemical Performance of the Composite Electrodes. Eur. Chem. Technol. J. 2016, 18, 3.
194. Pikalova, E.; Kolchugin, A.; Koroleva, M.; Vdovin, G.; Farlenkov, A.; Medvedev, D. Functionality of an Oxygen $Ca3Co4O9+\delta$ Electrode for Reversible Solid Oxide Electrochemical Cells Based on Proton-Conducting Electrolytes. J. Power Sources 2019, 438, 226996.
195. Filonova, E.A.; Tokareva, E.S.; Pikalova, N.S.; Vylkov, A.I.; Bogdanovich, N.M.; Pikalova, E.Y. Assessment of Prospective Cathodes Based on $(1 - x)Ca3Co4O9+\delta - xBaCe0.5Zr0.3Y0.1Yb0.1O3 - \delta$ Composites for Protonic Ceramic Electrochemical Cells. J. Solid State Electrochem. 2020, 24, 1509–1521.

Retrieved from <https://encyclopedia.pub/entry/history/show/106661>